Particle swarm optimization for simultaneous analysis of Magnetotelluric (MT) and Time Domain EM (TDEM) data

(Article begins on next page)

19 April 2024

Particle swarm optimization for simultaneous analysis of magnetotelluric and time-domain electromagnetic data

Alessandro Santilano[1], Alberto Godio[2], and Adele Manzella[1]

ABSTRACT

We have developed an innovative, simultaneous 1D optimization of electromagnetic (EM) data. Our scheme is suitable for the simultaneous analysis of magnetotelluric (MT) and time-domain EM (TDEM) data based on the probabilistic and evolutionary particle swarm optimization (PSO) algorithm. The simultaneous optimization also identifies and removes the static shift from the MT data. In our scheme, the static shift of the MT apparent resistivity curve is considered as an additional parameter S to be optimized. We tested the suggested method on the synthetic data and then applied it to the data from an EM geophysical study carried out in the geothermal area of Larderello-Travale (Tuscany, Italy). Apart from the novelty of using the PSO algorithm to estimate the model parameters by joint analysis, the simultaneous optimization of the static shift parameter addresses a major problem in MT, i.e., how to define and remove the galvanic effects on MT curves according to independent information, such as that provided by TDEM data. The procedure is expected to strongly influence the application of MT, particularly in geothermal exploration, which commonly relies extensively on EM methods.

INTRODUCTION

We describe an integrated data analysis method for the simultaneous optimization of magnetotelluric (MT) and time-domain electromagnetic (TDEM) soundings. We demonstrate that the method can effectively minimize the inherent static shift problem commonly encountered in MT data acquisition, while also increasing the accuracy and resolution of the 1D interpretation of EM soundings. We discuss the application of the particle swarm optimization (PSO) algorithm, a

heuristic method based on evolutionary and adaptive principles. The strength of this approach is that the global minimum of the minimization function can be reached without relying on a starting model that can influence the model parameters' estimations. Furthermore, the direct minimization of the function allows for the easy setting of simultaneous optimization of different data sets and the use of external constraints. The stochastic influence can also be used to retrieve information on the uncertainties of the results, by analyzing the a posteriori distribution of solutions.

MT and TDEM are geophysical methods commonly used for the indirect imaging of subsurface electrical resistivity. For a complete description of their theoretical basis, readers are referred to Tikhonov (1950), Cagniard (1953), Ward and Hohmann (1988), Spies and Frischknecht (1991), and to the reviews by Chave and Jones (2012) and Spichak (2015).

The "static shift" galvanic distortion of MT data is caused by near-surface small-scale heterogeneities or topography. The effect is a frequency-independent shift of the MT apparent resistivity curve for an unknown multiplier (constant on a logarithmic scale) that does not affect the MT phase (Jones, 1988). In a review of the distortion effects in MT, Jones (2012) considers the distortion of regional electric fields by local structures to be the greatest problem. Our work is intended to help overcome this problem by providing a quantitative estimate of the static shift using PSO optimization.

We first describe the state of the art on the integration of different EM data sets for overcoming the static shift in MT and a brief introduction to the probabilistic approach for solving the geophysical inverse problem. We discuss the PSO algorithm and apply it to the simultaneous optimization of MT and TDEM soundings. We also discuss the minimization functions implemented for estimating the model parameters and for removing the static shift of the MT curve. The novelty of the approach lies in the application of a global optimization algorithm to solve the MT inverse problem with the joint use of TDEM data and the use of the static shift of the MT apparent resistivity curve as an additional parameter S to be optimized.

[1]CNR-IGG, National Research Council, Pisa, Italy. E-mail: alessandro.santilano@igg.cnr.it; adele.manzella@igg.cnr.it.
[2]DIATI-Politecnico di Torino, Torino, Italy. E-mail: alberto.godio@polito.it.

We begin by testing our approach on synthetic data sets to properly simulate the static shift effects, and we then apply it to an experimental data set derived from an EM survey carried out in the geothermal area of Larderello (Tuscany, Italy) as part of the EU-FP7 IMAGE Project, a European project dedicated to generating innovative and integrated geothermal exploration methods.

State of the art on TDEM and MT joint analysis

Various schemes have been proposed for the joint analysis of EM data sets such as MT and controlled-source electromagnetic (CSEM) (Commer and Newman, 2009; Abubakar et al., 2011), TDEM and MT data sets (e.g., Sternberg et al., 1988; Pellerin and Hohman, 1990; Meju, 1996) and for simultaneous inversion of different parameters in EM problems (e.g., Kennet et al., 1988; Li et al., 2016). Since the late 1980s, the TDEM method has proved to be an effective means of correcting the static shift of distorted MT data because TDEM measurements are not affected, or are only affected very slightly, by such distortions. Among the various approaches for such correction, the scientific community still relies on joint TDEM and MT analysis for geothermal exploration (e.g., Arnason, 2015), the two methods being widely used for imaging geothermal systems (Spichak and Manzella, 2009; Muñoz, 2014; Santilano et al., 2015).

Pellerin and Hohman (1990) describe a correction scheme for the MT static shift based on the 1D inversion of TDEM data acquired from the same MT site. The idea is simple and effective for identifying the static shift of the 1D MT response. The procedure implies the inversion of the TDEM data (which are not affected by galvanic distortion) and the computation of the theoretical MT response of the TDEM 1D inversion model, to be used as the reference apparent resistivity for the shallow part of the investigated earth. The static shift is identified by comparing the reference MT curve (usually at frequencies >1 Hz) and the measured MT apparent resistivity curve. The shift is then removed by manually shifting the distorted MT curve to fit the undistorted, reference MT curve. The authors propose synthetic examples in 1D and 3D settings.

Sternberg et al. (1988) propose a quite different approach that directly compares the values of apparent resistivity, obtained from the MT and central-loop TDEM soundings. The method is mainly based on the correlation between the time-domain diffusion depth and the frequency-domain skin depth. At a certain site and at the same depth of penetration, the TDEM time (t) is assumed to be equivalent to the MT period (T) according to the following equality (Sternberg et al., 1988):

$$t = 194/f, \qquad (1)$$

where t(s) is the TDEM time and f(Hz) is the MT frequency. Therefore, the TDEM response is converted into an equivalent MT period by multiplying the time of the TDEM signal by the conversion factor, as proposed in equation 1. The MT curve is manually shifted in accordance with the apparent resistivity curve of the TDEM. Obviously, the overlapping of the two apparent resistivity curves (TDEM, MT) occurs only for the longer periods of the TDEM curve, due to the shallower investigation depth of the converted TDEM with respect to MT.

Meju (1996) proposes a method for constraining the MT soundings in a joint inversion scheme with the TDEM data, which does not require static shift correction in the preprocessing of the MT data. The method is based on a joint least-squares solution to the inverse problem. Briefly, the author took into consideration the apparent resistivity of the TDEM and the phase of MT in the discrepancy vectors and the matrices of partial derivatives, both of which are unaffected by static shift; the MT apparent resistivity is neglected in the joint inversion being distorted.

THE PROBABILISTIC APPROACH IN EM OPTIMIZATION

In EM geophysics, a complete understanding of the physics behind the method allows the measured data to be related to the model parameters of the earth. The inverse problem is to find the model parameters $\mathbf{m}$, given certain observed data $\mathbf{d}$ (Tarantola, 2005; Menke, 2012; Aster et al., 2013):

$$F(\mathbf{m}) = \mathbf{d_{obs}}, \qquad (2)$$

where the forward functional F describes the physical process of EM induction. By solving the inverse problem, the geophysicist indirectly estimates the physical parameters of the subsoil (i.e., the resistivity model of the investigated earth) from the analysis of the EM data measured at the surface. The problem in MT is ill-posed due to its instability (Berdichevsky and Dmitriev, 2002).

The methods for solving the inverse problem can be classified into deterministic and probabilistic methods. Deterministic methods are the conventional means of estimating the resistivity models. Because the MT response is particularly affected by dimensionality, the literature is rich in deterministic schemes for 1D, 2D, and 3D inversions, with 3D inversion being the main focus of current scientific research. The joint-inversion problem in geophysics (e.g., De Nardis et al., 2005; Linde and Doetsch, 2016), and particularly in MT (e.g., Moorkamp et al., 2011; Bastani et al., 2012), is a current scientific challenge. In general, the model parameters are solved iteratively by minimizing a functional operator according to a derivative approach. The procedure may reach a local minimum of the functional operator, depending also on how close the starting model is to the global minimum. Two of the most common schemes for applying the deterministic approach in EM are Occam's inversion (Constable et al., 1987; Degroot-Hedlin and Constable, 1990) and the nonlinear coniugate gradients method (Rodi and Mackie, 2001). Despite theoretical demonstrations, in practice, the MT inverse problem is nonunique, mainly due to the effect of noise, the finite number of frequencies (Grandis et al., 1999), and anisotropy (Yin, 2003). For a mathematical review of MT inversion algorithms, see Siripunvaraporn (2012).

Conversely, the probabilistic approach is less conventional and is still being researched. The probabilistic methods do not imply any derivative approach, but the model space is sampled randomly or according to some strategy. Moreover, this approach does not need a starting model that can influence the success of the inversion procedure.

In the probabilistic methods, many earth models are proposed and the theoretical data are compared with the observed data. The minimization function is directly estimated to retrieve the best model. The philosophy of the probabilistic approach, which can be considered as an optimization procedure, is to explore a wider space solution to seek a global solution to the problem. For instance, Monte Carlo methods are based on the concept of random sampling of the model space (Metropolis and Ulam, 1949). Moreover, various schemes, known as global optimization algorithms, are available in

the literature; for a complete description of the application of such methods in geophysics, we refer readers to Sen and Stoffa (2013).

In recent decades, computational intelligence algorithms based on the concept of adaptive behavior have been proposed to solve nonlinear problems. Such applications have also been used to solve the geophysical inverse problem. Common algorithms are (1) genetic algorithms, (2) simulated annealing, and (3) PSO (Holland, 1975; Kirkpatrick et al., 1983; Kennedy and Eberhart, 1995). The adoption of such global optimization algorithms for solving the MT inverse problem was proposed in literature (e.g., Dosso and Oldenburg, 1991; Everett and Schultz, 1993; Shaw and Srivastava, 2007), mostly by using genetic algorithms and simulated annealing.

The PSO algorithm

Kennedy and Eberhart (1995) present the heuristic PSO method. Despite its widespread use in engineering, few applications have been proposed in geophysics (e.g., Fernández Martínez et al., 2010a, 2010b) and fewer in MT (e.g., Shaw and Srivastava, 2007). We adopt the PSO algorithm with the aim of retrieving information from the simultaneous optimization of TDEM and MT data. We provide only the basics of the method because a detailed description of the algorithm and its application to MT is not the focus of this paper; for further details, we refer readers to Godio et al. (2016) and Godio and Santilano (2018).

PSO is based on two main concepts: (1) the simulation of swarm intelligence and the behavior of flocks of bird and fish and (2) evolutionary computation. The swarm represents a population of earth models. The elements (or "particles") that make up the swarm explore the solution space of the problem. At each iteration, the PSO updates the model parameters of the swarm through adaptive behavior. The movement of particles in the solution domain is not entirely random. Each particle is attracted toward its own personal best position, in terms of the fitness of the solution, and the best particle position for the swarm. The position of a particle is updated at each iteration by adding a displacement vector called velocity. Following Engelbrecht (2007), the velocity consists of three terms: cognitive, social, and inertia. The cognitive component holds the experience of the individual particles, the social component holds shared information about the swarm's best solution, and the inertia component represents the previous position in the space domain (Engelbrecht 2007).

For the 1D optimization of EM (TDEM and MT) data, the N-dimensional space of admissible earth models j is defined. For the kth parameter of the jth model, the lower and upper limits l_k and u_k of the search domain as well as the number of model parameters and particles, are set a priori. Depending on the function to be minimized, the model parameters k may be the resistivities ρ and thicknesses, or only the resistivities (with fixed thicknesses) of a layered earth.

The algorithm updates positions $\mathbf{x_j}(t)$ and velocities $\mathbf{v_j}(t)$ of the individuals as follows (Engelbrecht, 2007):

$$\mathbf{v_j}(t+1) = \varpi\mathbf{v_j}(t) + c_1 r_1 (\mathbf{l_j}(t) - \mathbf{x_j}(t)) \\ + c_2 r_2 (\mathbf{g}(t) - \mathbf{x_j}(t)). \quad (3)$$

$$\mathbf{x_j}(t+1) = \mathbf{v_j}(t+1) + \mathbf{x_j}(t). \quad (4)$$

At the tth iteration ($t = 0 \ldots T$, where T is the maximum number of generations), each particle j of the swarm samples the search space according to its own misfit history $\mathbf{l_j}(t)$ and its companions' search experience $\mathbf{g}(t)$. The coefficients ω, c_1, and c_2 are the inertia weight, the cognitive attraction, and the social attraction, respectively. The random values r_1 and r_2 impose a stochastic influence on the displacement updating.

PSO minimization function for MT data

The optimization process for estimating the model parameters from the MT soundings focuses on the discussion of the function to be minimized. The minimization function Ψ usually consists of different terms (e.g., Aster et al., 2013; Sen and Stoffa, 2013). The different functions that can be used for the 1D optimization of MT data are described in detail by Godio and Santilano (2018).

For every particle of the swarm, at each iteration, the solution of the forward problem is computed according to a nonlinear forward functional $F(j)$. The PSO optimization process evaluates the proposed models through the minimization function dependent on the computed theoretical response $F(x)$ and observed data $\mathbf{d}$.

We adapt the approach suggested by Smith and Booker (1988) by minimizing the structure. In the deterministic schemes, the minimum structure is measured in terms of the derivative of the model. Herein, we adopt a minimization function that follows the "Occam-like" regularization proposed by Constable et al. (1987). We aim to minimize the roughness of the model. To achieve a "smooth" model, PSO is applied to the MT data by minimizing the following general function:

$$\Psi(\mathbf{m}) = (a\|\boldsymbol{\rho_{a,o}} - \boldsymbol{\rho_{a,p}}\|_2 + b\|\boldsymbol{\phi_{a,o}} - \boldsymbol{\phi_{a,p}}\|_2) + \lambda\|\partial\mathbf{m}\|_2. \quad (5)$$

The first term of equation 5 is related to the data misfit, or the Euclidean (data) norm of the misfits between the observed experimental data $\boldsymbol{\phi}$-$\boldsymbol{\rho_{a,o}}$ and the theoretically predicted data $\boldsymbol{\phi}$-$\boldsymbol{\rho_{a,p}}$; the symbols ϕ_a and ρ_a refer to the MT phase and the apparent resistivity, respectively. The model roughness represents the second term of equation 5, and it is computed by applying a differencing operator to the elements of the model vector $\mathbf{m}$; a Lagrangian multiplier λ is applied to weight the relevance of the smoothing on the data fitting. In the Occam optimization, the vector of model parameters $\mathbf{m}$ consists only of the electrical resistivity values for a many-layered earth model with fixed thicknesses. This approach looks for the smoothest possible model that fits the observed data. The swarm particles (i.e., the proposed resistivity models) are evaluated according to equation 5. The model parameters of the particles are updated at each iteration, according to equations 3 and 4.

SIMULTANEOUS OPTIMIZATION OF TDEM AND MT SOUNDINGS: TEST ON SYNTHETIC DATA

Simultaneous TDEM and MT model parameter estimation from PSO optimization

We first describe a test using synthetic data from a 1D layered earth without any distortion of the MT data. In this case, we apply the PSO to a joint data set in the frequency domain composed of the MT data and the converted TDEM data according to equation 1, as proposed by Sternberg et al. (1988). We slightly modify the general minimization function, equation 5, for the Occam-like solution with PSO by considering an additional term to minimize the Euclidean

norm of the misfits between the converted TDEM apparent resistivity $\rho_{a(TDEM),o}$ and the theoretically predicted data $\rho_{a(TDEM),p}$. The minimization function for simultaneous optimization is

$$\Psi(\mathbf{m}) = (a\|\rho_{a,o} - \rho_{a,p}\|_2 + b\|\phi_{a,o} - \phi_{a,p}\|_2 + c\|\rho_{a(TDEM),o} - \rho_{a(TDEM),p}\|_2) + \lambda\|\partial m\|_2. \tag{6}$$

The symbols ϕ_a and ρ_a refer to the MT phase and the apparent resistivity, respectively. The minimization function allows us to weight the contributions of the different data, i.e., the MT apparent resistivity and phase, and the TDEM apparent resistivity, using a, b, and c coefficients.

We consider a simple four-layered synthetic model (model 1) with the following thicknesses and resistivity values: 200 m and
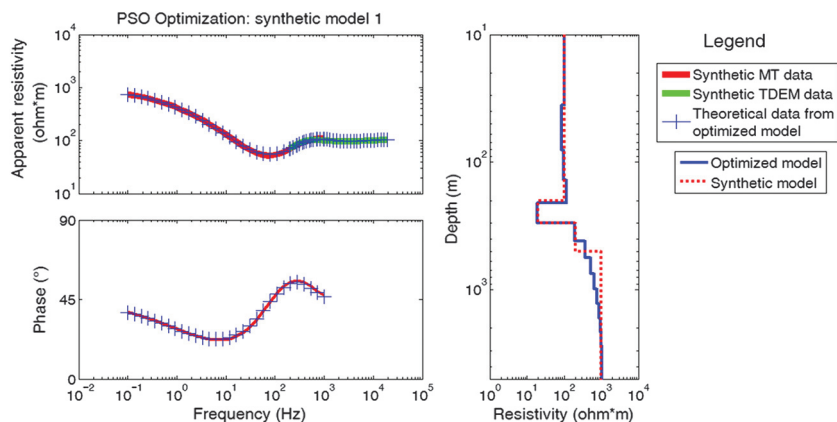

Figure 1. Optimization results of the synthetic data from model 1. The joint data set is composed of apparent resistivities and phases of the MT and the apparent resistivities of the TDEM.

Table 1. Main settings for the PSO-Occam optimization of the synthetic data set (model 1).

PSO (Occam-like): lower boundary (LB)/upper boundary (UB)		
Number of layers to be optimized	Resistivity (ohm m)	Thickness
19	LB = 1; UP = 2000	Log. increase from 35 m
PSO: Settings		
Initial population	300	
Particle inertia	0.9	
Cognitive attraction	0.75	
Social attraction	1.75	
Generations (iterations)	200	
Trials	1	
PSO: Objective function		
a, weight on ρ_a	0.8	
b, weight on Φ	0.2	
c, weight on $\rho_{a(TDEM)}$	1	
λ (Lagrangian multiplier)	10^{-3}	

100 Ωm, 100 m and 20 Ωm, 200 m and 200 Ωm, and a half-space of 1000 Ωm (see the synthetic model in Figure 1). The MT theoretical data are computed in the frequency range of 0.1–1000 Hz using forward modeling based on a recursive formula for computing the surface impedance Zi at the top of each ith layer, as described by Sims and Bostick (1969) and Pethick and Harris (2015). The TDEM forward problem is solved for a central-loop configuration, as proposed by Ingeman-Nielsen and Baumgartner (2006), on the basis of the Hankel transforms in the field equations. MT and TDEM data are not perturbed by noise. The TDEM times are converted into MT frequencies, in the range of 194–19,400 Hz, using the conversion coefficient of equation 1. We summarize the main features of the optimization in Table 1.

The earth model is discretized as a function of the frequency of the measured EM fields. It includes 19 layers that increase in thickness in logarithmic increments, according to the skin depth concept. The model parameters to be optimized are the resistivities of each layer. The lower and upper boundaries of resistivity for each layer are properly set in the range of 1–2000 Ωm, i.e., the space domain to be sampled for the solution of the inverse problem. The inertia weight, the cognitive attraction, and social attraction are 0.9, 0.75, and 1.75, respectively, whereas the Lagrangian multiplier λ is set to equal 10^{-3}. We consider a population size of 300 for the swarm, which means that 300 earth models are tested and optimized every 200 iterations. The best model, i.e., the model toward which the swarm converges, emerges at the end of the procedure. The procedure runs for many trials with the same features. This leads to the evaluation of the a posteriori distributions of the model parameters, and it provides a useful data set to test the statistical validity of the results (as described in the following sections). A single trial is enough to test model 1 due to the absence of noise. The resulting model, shown in Figure 1, validates the effectiveness of PSO for simultaneous optimization. The overlap between the two data sets is satisfactory (Figure 1).

Static shift removal and model parameter estimation from simultaneous PSO optimization

An important application of the simultaneous PSO of EM data is the resulting innovative method for identifying and removing the static shift from the MT data.

Considering MT and TDEM soundings measured at a certain site, the joint data set in the frequency domain is initially created by converting the TDEM data according to equation 1. Basically, the earth resistivity models are evaluated on the basis of the misfit between (1) the predicted MT phase and resistivity data $\phi_{a,p} - \rho_{a,p}$ and TDEM apparent resistivity $\rho_{a(TDEM),p}$ and (2) the observed TDEM apparent resistivity, the MT phase, and the MT apparent resistivity, the latter multiplied by the shift parameter S, which is a parameter to be optimized. The concept behind equation 7 is that the resistivity models are also tested with the measured MT apparent resistivity shifted for S (in the operation $S\,\rho_{a,o}$). That means a strong influence of this operation on the minimization, i.e., static shift S not in accordance with the TDEM curve causes worse values of the minimization functions. Being that S is continuously optimized according to

the PSO algorithm, the parameter is stochastically sampled with an evolutionary strategy to find the value of S that properly shifts the MT curve in accordance with the reference TDEM apparent resistivity (obviously fixed in the procedure). The best solution that provides the smoothest model and the proper static shift value in accordance with the reference TDEM converted curve is then obtained. The minimization function is described as

$$\Psi(\mathbf{m}) = (a\|(\mathbf{S}\boldsymbol{\rho_{a,o}}) - \boldsymbol{\rho_{a,p}}\|_2 + b\|\boldsymbol{\phi_{a,o}} - \boldsymbol{\phi_{a,p}}\|_2 + c\|\boldsymbol{\rho_{a(TDEM),o}} - \boldsymbol{\rho_{a(TDEM),p}}\|_2) + \lambda\|\partial\mathbf{m}\|_2. \quad (7)$$

To test the scheme on a synthetic data set that properly simulates the MT static shift, we use the synthetic MT data from Sternberg et al. (1988) that modeled the MT response for a shallow 3D body at a small scale in a 1D layered earth (hereafter, model 2). Figure 2 shows the features of the synthetic model and the galvanic distorted and undistorted MT curves that simulate the acquisition above a surface inhomogeneity and at an infinite distance (i.e., the 1D response). The TDEM synthetic data are computed for a 150-m central-induction sounding using the algorithm proposed by Ingeman-Nielsen and Baumgartner (2006). The MT data set is forward modeled in the frequency range of 100–0.001 Hz. The TDEM data set is modeled in a time range of 0.1–1000 ms because the response is unaffected by the inhomogeneity in this time range, as pointed out by Sternberg et al. (1988).

The static-shifted MT apparent resistivity curve is shifted by about a decade in the logarithmic scale compared with the undistorted curve. We test the effectiveness of the PSO procedure by considering the minimization function in equation 7. The main features of the optimization of model 2 are summarized in Table 2.

The upper and lower boundaries for setting the search domain of S are in the range of 0.001–10, whereas the search domain of the resistivity of layers is in the range of 1–2000 Ωm. With respect to model 1, in this optimization we increase the weight of the phase in the minimization function to 0.5. The procedure is repeated for 25 trials using the same settings to test the repeatability of the results. The resulting a posteriori distribution is very useful for identifying layers with scattered results that indicate poor quality results.

Figure 3 shows the results of the optimization and the reference model among the 25 trials, which is the model with the lowest normalized rms. In addition to the validity of the resulting resistivity model, we underline the proper optimization of the static shift by retrieving the correct value with reference to the TDEM "converted" curve (Figure 3).

APPLICATION OF THE SIMULTANEOUS OPTIMIZATION TO THE MEASURED DATA: A CASE STUDY OF THE LARDERELLO GEOTHERMAL FIELD (ITALY)

TDEM and MT data sets

To test the stochastic simultaneous analysis of the TDEM and MT data sets on real data contaminated by galvanic distortion,

we apply the proposed method to an EM data set from a survey carried out in the geothermal area of Larderello-Travale (Tuscany, Italy). The acquisition of MT and TDEM soundings was carried out in the frame of a European project (EU FP7) called IMAGE Project aimed at developing integrated and novel methods for geothermal exploration (Santilano et al., 2016). The TDEM soundings in the area were acquired at the same sites as the selected MT soundings. We briefly describe the data set before focusing on the joint analysis of the EM data.

In 2016, 22 broadband MT soundings were acquired using the Zonge system (Figure 4). Due to various cultural sources of noise that perturbed the naturally occurring MT signals, in particular those created by DC electrified railways, a remote reference tech-
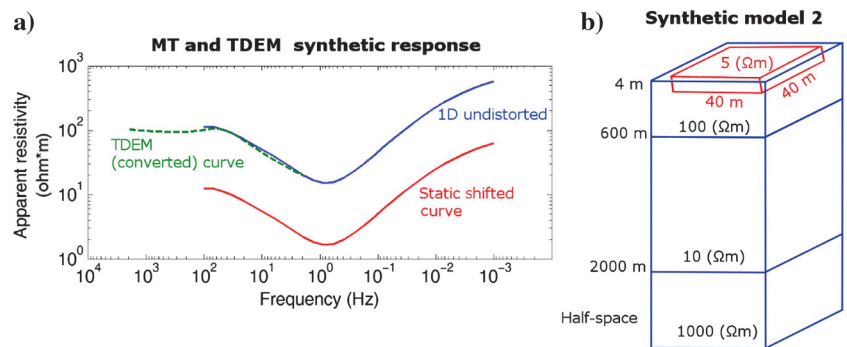

Figure 2. Synthetic model 2 for simulating the static shift of MT curves. (a) The theoretical data for a central-loop (150 m) TDEM sounding and the MT data. (b) The 1D model and the surface thin 3D volume that causes the inhomogeneity and produces the static-shifted MT curves. The model and the MT data are from Sternberg et al. (1988).

Table 2. Main setting for the PSO-Occam optimization of the synthetic data set (model 2).

PSO (Occam-like): LB/UB		
Number of layers to be optimized	Resistivity (ohm m)	Thickness
19	LB = 1; UB = 2000	Log. increase from 112 m
Additional parameter to be optimized	**Value of shift**	
Static shift S	LB = 0.001; UB = 10	
PSO: Settings		
Initial population	300	
Particle inertia	0.9	
Cognitive attraction	0.75	
Social attraction	1.75	
Generations (iterations)	200	
Trials	25	
PSO: Objective function		
a, weight on $\boldsymbol{\rho_a}$	0.5	
b, weight on Φ	0.5	
c, weight on $\boldsymbol{\rho_{a(TDEM)}}$	1	
λ (Lagrangian multiplier)	10^{-3}	

nique (Gamble et al., 1979) was used to process data. The remote site was installed on the volcanic Isle of Capraia (Italy). The MT stations were laid out in an L-shaped configuration to measure the four components of the MT fields (Ex, Ey, Hx, Hy), with a dipole length of 100 m. The MT tensor was further decomposed as proposed by LaTorraca et al. (1986). The dimensionality analysis, as proposed by Marti et al. (2005), highlighted a complex 3D structure for these soundings.

After estimating the transfer function of the MT soundings, we selected 10 sites that showed clear static shift effects, for the acquisition of TDEM data. The equipment was a TEM-FAST 48 (AEMR company; for details, see Ranieri, 2000; Barsukov et al. 2015). The TDEM soundings were acquired by laying out a 100×100 m rectangular

loop of wire and pulsing it with a controlled current. The configuration was a coincident loop; i.e., the same loop was used for transmitting and receiving. The acquisition system was set to transmit a current of up to 3 A with active time gates from 4 μs to 2.024 or 4.048 ms and a stacking time of a few minutes. The ratio of "current on" to "current off" time was 3 to 1. The time window (current off time) extended from 4 μs to 4 ms with 48 signal integration channels.

Results of the simultaneous optimization from selected sites

We apply the proposed simultaneous optimization to the analysis of the real data set and to correct the static shift of MT data while retrieving 1D preliminary information on the resistivity distribution. The optimization is also challenging because of the particularly high level of noise in the data. Many of the acquired MT curves show a strong static shift, probably due to the shallow heterogeneities and the topography. The geology of the area is quite complex due to the polyphased tectonics that affects this sector of the Apennine belt; the high-temperature hydrothermal circulation in this long-lived geothermal system also influences the geophysical response.

Here, we refer to one MT site, "Lard_16." The MT sounding resulted noisy and the frequency range of $256 – 3 \times 10^{-2}$ Hz was considered. The TDEM data acquired from the same site in the time range of 5.26×10^{-5} to 4.7×10^{-3} s showed a very low level of noise.

We follow the procedure described above and minimize equation 7 to optimize the resistivities of a smooth model and the static shift parameter S. Our aim in this third case was to solve the static shift problem of a real MT sounding and retrieve preliminary resistivity information, albeit limited to 1D in a 3D environment.

In the third optimization, we maintain the same number (25) of trials as in the second test and enlarge the search domain of the static shift S to guarantee a global search. The value of cognitive attraction is increased, while reducing that of social attraction. We also increase the number of model layers from 19 to 29. We show the results for the yx component of the "Lard 16" sounding in Figure 5.

Figure 5 shows the optimal fit of the MT and TDEM curves after retrieving the S (static shift) parameter.

We evaluate the a posteriori distribution by running the procedure several times. The a posteriori analysis could be useful for identifying poor results related to the optimized model parameters (static shift S or layer resistivities), in terms of a scattered versus normal distribution. For example, the a posteriori analysis of the 25 trials shows a normal distribution of the parameter S (Figure 6) and the resistivities of the shallow layers (Figure 7 shows the third layer
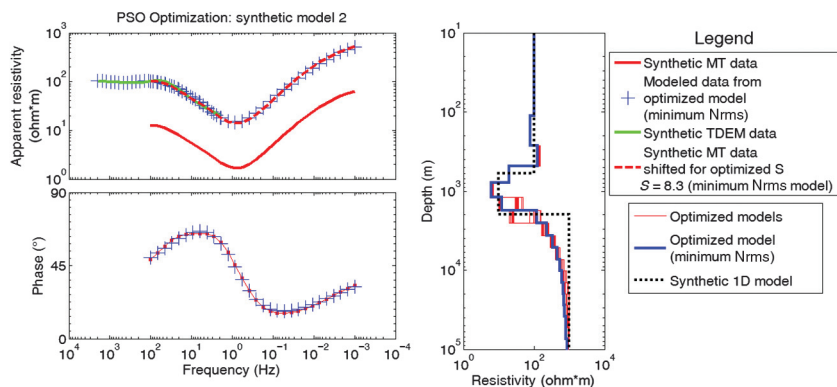

Figure 3. The PSO optimization of synthetic model 2. The resulting 25 models are shown in red, and the minimum normalized rms model is shown in blue. The theoretical MT data are shown (on the left) for the minimum normalized rms model and compared with the synthetic MT and TDEM data. The MT apparent resistivity curve multiplied by the optimized S is also shown.
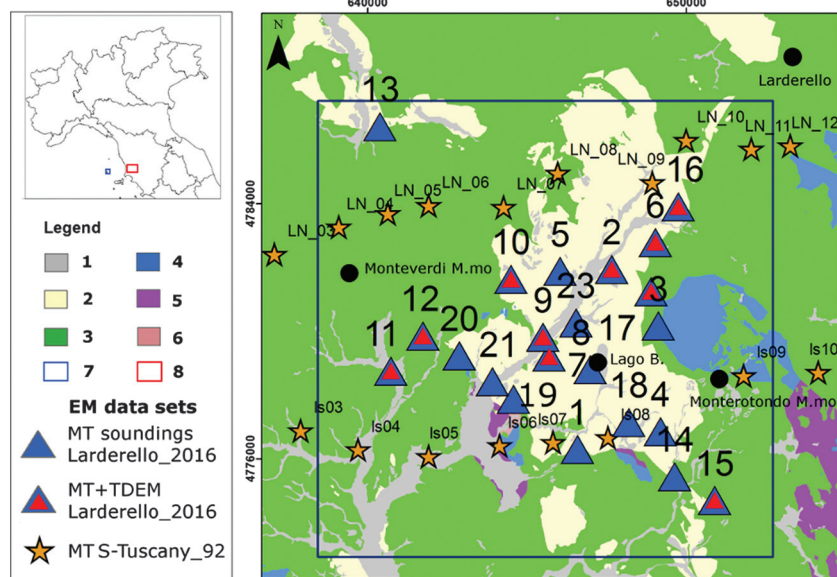

Figure 4. Location of the MT and TDEM soundings of previous (S-Tuscany_92) and new data sets available for the study area: (1) quaternary deposits, (2) neoautochthonous terrigenous deposits (Miocene-Pliocene), (3) Ligurian and sub-Ligurian Flysch complex (Jurassic-Eocene), (4) Tuscan Nappe formations (Upper Trias-Miocene), (5) Calcare Cavernoso and anhydrites, (6) metamorphic units (Paleozoic), (7) remote MT site on the Island of Capraia, and (8) surveyed area within the Larderello geothermal field.

results), whereas the central layers of the model show a more scattered resistivity distribution, indicating poor results (Figure 8 shows the results for layer 15). The standard deviations are 0.4 and 136 for layers 3 and 15, respectively.

DISCUSSION

We tuned the PSO settings in various tests, to check the effectiveness of the evolutionary approach for the simultaneous optimization of TDEM and MT data and to obtain a quantitative estimate of the MT static shift. The tests on synthetic data sets proved the suitability of the PSO algorithm for optimizing the model parameters of a 1D layered earth and for identifying and removing the static shift effects in MT data based on the converted TDEM apparent resistivity curves.

In the first test on synthetic model 1, we minimized equation 6 by adding a term related to the TDEM apparent resistivity, to obtain the best solution for a smooth earth model, similar to the Occam inversion. At very high frequencies, higher than 1000 Hz, the data misfit refers only to the TDEM curve converted into the frequency domain according to equation 1. At frequencies in the range of 194–1000 Hz, the data refer to TDEM and MT apparent resistivity and also to the MT phase. The coefficients a, b, and c weight the single contribution. In the absence of noise in the case of model 1, the test results using different coefficients are similar and consistent; here, we present the results according to the settings summarized in Table 1. The match between the emerged earth resistivity model obtained by PSO optimization and the synthetic model we proposed for the test is striking. The reduced sensitivity to match the depth of the half-space was on the order of a few meters.

In the second test on synthetic model 2, we minimized equation 7 by adding the static shift of the MT curve as a parameter S to be optimized. The synthetic data, obtained by simulating the effects of shallow conductive inhomogeneity in a 1D earth, represent an ideal context for testing the quality of the proposed method. Conceptually, the approach is quite simple in the sense that the predicted MT apparent resistivities of the thousands of computed models are compared with the "measured" MT curve multiplied by a static shift parameter that is continuously updated based on the adaptive PSO behavior. The results in Figure 3 clearly show that, at least for a 1D earth structure, the proposed procedure is very effective for optimizing the resistivity of a smooth model and the static shift by the simultaneous analysis of TDEM and MT soundings. Similar to the first test model, we observe a lower sensitivity to sharply define the depth of the half-space, which is a layer with high resistivity. The parameter S, related to the galvanic shift of the MT data, is perfectly retrieved according to the reference TDEM curve. It is worth underlining that at the end of the optimization, the algorithm provides the best model, i.e., the model toward which the swarm converges. It is good practice to run several trials so that the a posteriori distribution can be analyzed to identify scattered distributions of single parameters (e.g., the resistivity of a layer), which indicate poor results. In our case, we ran the PSO 25 times

using the same settings as summarized in Table 2 and found that the distribution of the optimized parameters was normal.

The application of the procedure to the analysis of a real measured EM data set acquired as part of a scientific geothermal project in the Larderello geothermal field (Italy) was quite challenging. The level of data noise was high, as is often the case in geothermal exploration. Although the lowest periods of the MT sounding were neglected in our test, the merged MT/TDEM apparent resistivity curve covered a broad band ranging from 8×10^{-1} to almost 4×10^{3} Hz. To overcome the uncertainties due to the noise in
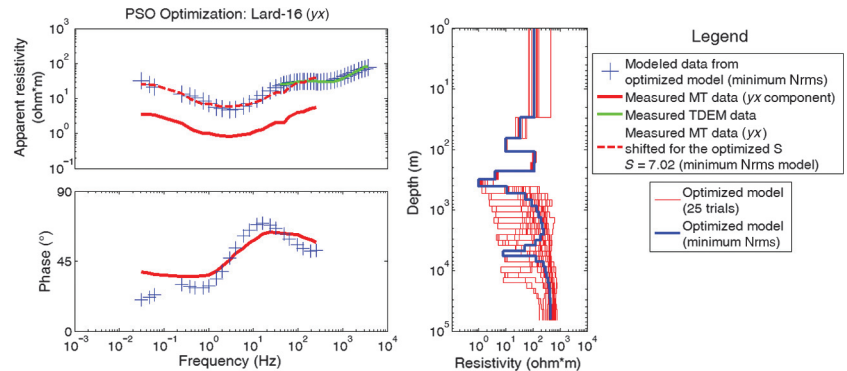

Figure 5. The PSO optimization of the Lard_16 measured MT sounding (YX mode). The resulting 25 models are shown in red, and the minimum normalized rms model is shown in blue. The theoretical MT data are shown (on the left) for the minimum normalized rms model and compared with the measured MT and TDEM data. The measured MT curve multiplied by the optimized S is also shown.
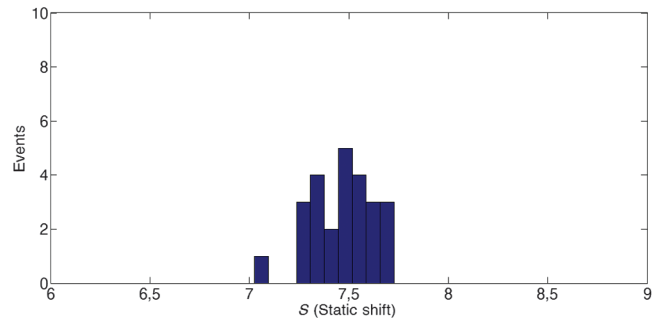

Figure 6. A posteriori distribution of the optimized parameter S (static shift) among 25 PSO trials on the Lard_16 measured MT sounding.
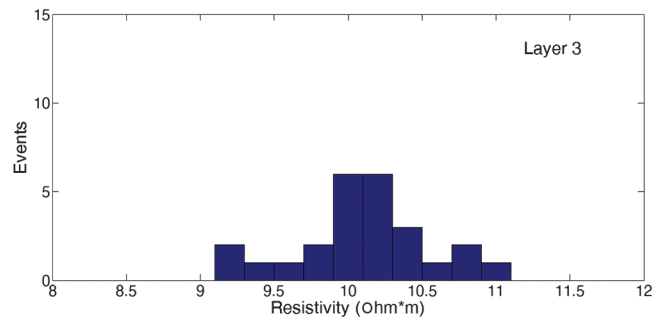

Figure 7. A posteriori distribution of the resistivity of layer 3 from the simultaneous PSO on the Lard_16 measured MT sounding.

the data, it was possible to increase the swarm population and the generations (see Table 3), despite the higher computation time. The results of our third test, shown in Figure 5, confirm the efficacy of our method for identifying and removing the static shift in the MT data. The best of the 25 models, i.e., the one with the lowest normalized rms, was obtained when $S = 7.02$. The a posteriori distribution in Figure 6 shows very good results for the optimization of the static shift parameter S, with values in the range of 7.02–7.72 for a search domain in the range of 0.001–100. The a posteriori analysis also showed very consistent results when retrieving the resistivity of the shallow layers (Figure 7) and poor-quality results for the central layers (Figure 8). This latter scattered distribution may be due to the propagation of the data noise that was evident, for example, in the MT phase that could not be properly fitted. The difference between the distributions is evident in Figures 7 and 8: the resistivity
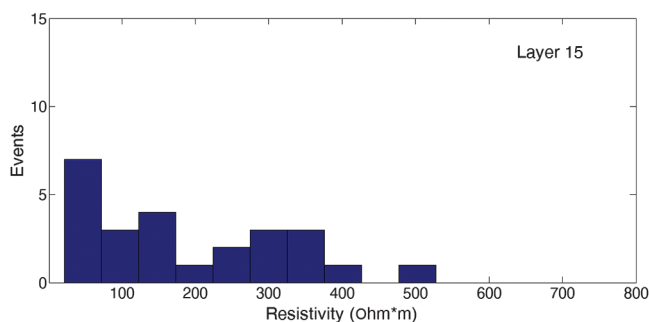

Figure 8. A posteriori distribution of the resistivity for layer 15 from the simultaneous PSO of the Lard_16 measured MT sounding.

Table 3. Main settings for the PSO-Occam optimization of the Lard-16 sounding.

PSO (Occam-like): LB/UB		
Number of layers to be optimized	Resistivity (ohm m)	Thickness
29	LB = 1; UB = 1000	Log. increase from 30 m
Additional parameter to be optimized	**Value of shift**	
Static shift S	LB = 0.001; UB = 100	
PSO: Settings		
Initial population	500	
Particle inertia	0.9	
Cognitive attraction	1	
Social attraction	1.5	
Generations (iterations)	250	
Trials	25	
PSO: Objective function		
a, weight on ρ_a	0.3	
b, weight on Φ	0.7	
c, weight on $\rho_{a(TDEM)}$	1	
λ (Lagrangian multiplier)	5×10^{-4}	

distribution for layer 3 is confined in the range of approximately 9–11 Ωm, whereas that for layer 15 is in the range of approximately 10–500 Ωm. Due to the higher dimensionality of the investigated earth's structure, the resulting optimized resistivity model should only be considered as preliminary information.

In the various tests on synthetic and real data sets, we acted on the population size (the number of particles in the swarm), on the social and cognitive attraction parameters and on the weight of the data (TDEM, MT apparent resistivity and phase) in the optimization. Setting these parameters allowed us to control the speed of convergence versus the capability to widely explore the solution search domain. Considering that an Occam optimization usually requires more than 20 parameters to be solved, the population and generation sizes must be carefully chosen. In our case, we achieved good convergence by selecting a population size of between 200 and 500 with 150–250 iterations, depending on the adopted number of layers (25–30).

Finally, it should be mentioned that this procedure is more time consuming than deterministic ones. Each test lasted approximately 4 min using a laptop with 8 GB of RAM and an Intel Core i7, which is a longer time with respect to a deterministic inversion taking a few seconds to be computed. However, this is just a temporary disadvantage that will be solved by computational technology progress, and it is concurrent to the many advantages already described.

CONCLUSION

The scheme proposed in this paper is suitable for the simultaneous analysis of MT and TDEM data based on PSO, a probabilistic and evolutionary algorithm.

In addition to the novelty of using the PSO algorithm to estimate the model parameters in a joint analysis, the method is also able to simultaneously optimize the static shift parameter, and hence to remove the galvanic effects on MT curves with reference to the independent TDEM data. Considering that TDEM and MT methods are commonly used in geothermal exploration due to the peculiar resistivity features of geothermal systems, this procedure could be very influential on geothermal exploration activity.

The application of simultaneous PSO optimization for obtaining an optimized earth resistivity model has been up till now limited to the one dimension. The possibility of analyzing the a posteriori distribution is a highly important development in the analysis of MT data. This kind of analysis is suitable for identifying resistivity layers that are poorly resolved due to high levels of noise or to intrinsic lower sensitivity of the EM method to the specific features.

ACKNOWLEDGMENTS

REFERENCES

Abubakar, A., M. Li, G. Pan, J. Liu, and T. M. Habashy, 2011, Joint MT and CSEM data inversion using a multiplicative cost function approach: Geophysics, **76**, no. 3, F203–F214, doi: 10.1190/1.3560898.
Arnason, K., 2015, The static shift problem in MT soundings: Proceedings of the 2015 World Geothermal Congress , 1–12.
Aster, R., B. Borchers, and C. H. Thurber, 2013, Parameter estimation and inverse problems: Elsevier.

Barsukov, P. O., E. B. Fainberg, and E. O. Khabensky, 2015, Shallow investigation by TEM-FAST technique: Methodology and examples, *in* V. V. Spichak, ed., Electromagnetic sounding of the earth's interior: Elsevier, 47–78.

Bastani, M., J. Hübert, T. Kalscheuer, L. B. Pedersen, A. Godio, and J. Bernard, 2012, 2D joint inversion of RMT and ERT data versus individual 3D inversion of full tensor RMT data: An example from Trecate site in Italy: Geophysics, **77**, no. 4, WB233–WB243, doi: 10.1190/geo2011-0525.1.

Berdichevsky, M. N., and I. V. Dmitriev, 2002, Magnetotellurics in the context of the theory of ill-posed problems: SEG.

Cagniard, L., 1953, Basic theory of the magnetotelluric method of geophysical prospecting: Geophysics, **18**, 605–635, doi: 10.1190/1.1437915.

Chave, A. D., and A. G. Jones, 2012, The magnetotelluric method, theory and practice: Cambridge University Press.

Commer, M., and G. A. Newman, 2009, Three-dimensional controlled-source electromagnetic and magnetotelluric joint inversion: Geophysical Journal International, **178**, 1305–1316, doi: 10.1111/j.1365-246X.2009.04216.x.

Constable, S. C., R. L. Parker, and G. C. Constable, 1987, Occam's inversion: A practical algorithm for generating smooth models from electromagnetic sounding data: Geophysics, **52**, 289–300, doi: 10.1190/1.1442303.

Degroot-Hedlin, C., and S. Constable, 1990, Occam's inversion to generate smooth, two-dimensional models from magnetotelluric data: Geophysics, **55**, 1613–1624, doi: 10.1190/1.1442813.

De Nardis, R., E. Cardarelli, and M. Dobroka, 2005, Quasi-2D hybrid joint inversion of seismic and geoelectric data: Geophysical Prospecting, **53**, 705–716, doi: 10.1111/j.1365-2478.2005.00497.x.

Dosso, S. E., and D. W. Oldenburg, 1991, Magnetotelluric appraisal using simulated annealing: Geophysical Journal International, **106**, 379–385, doi: 10.1111/j.1365-246X.1991.tb03899.x.

Engelbrecht, A. P., 2007, Computational intelligence, an introduction: John Wiley & Sons.

Everett, M. E., and A. Schultz, 1993, Two-dimensional nonlinear magnetotelluric inversion using genetic algorithm: Journal of Geomagnetism and Geoelectricity, **45**, 1013–1026, doi: 10.5636/jgg.45.1013.

Fernández-Martínez, J. L., E. García-Gonzalo, J. P. Fernández Álvarez, H. A. Kuzma, and C. O. Menéndez-Pérez, 2010a, PSO: A powerful algorithm to solve geophysical inverse problems. Application to a 1D-DC resistivity case: Journal of Applied Geophysics, **71**, 13–25, doi: 10.1016/j.jappgeo.2010.02.001.

Fernández-Martínez, J. L., E. García-Gonzalo, and V. Naudet, 2010b, Particle swarm optimization applied to solving and appraising the streaming-potential inverse problem: Geophysics, **75**, no. 4, WA3–WA15, doi: 10.1190/1.3460842.

Gamble, T. D., W. M. Goubau, and J. Clarke, 1979, Magnetotellurics with a remote reference: Geophysics, **44**, 53–68, doi: 10.1190/1.1440923.

Godio, A., A. Massarotto, and A. Santilano, 2016, Particle swarm Optimisation of electromagnetic soundings: 78th Annual International Conference and Exhibition, EAGE, Extended Abstracts, 1–5, doi: 10.3997/2214-4609.201602024.

Godio, A., and A. Santilano, 2018, On the optimization of electromagnetic geophysical data: Application of the PSO algorithm: Journal of Applied Geophysics, **148**, 163–174, doi: 10.1016/j.jappgeo.2017.11.016.

Grandis, H., M. Menvielle, and M. Roussignol, 1999, Bayesian inversion with Markov chains — I. The magnetotelluric one-dimensional case: Geophysical Journal International, **138**, 757–768, doi: 10.1046/j.1365-246x.1999.00904.x.

Holland, J. H., 1975, Adaptation in natural and artificial systems: University of Michigan Press.

Ingeman-Nielsen, T., and F. Baumgartner, 2006, CR1Dmod: A MATLAB program to model 1D complex resistivity effects in electrical and electromagnetic survey: Computers & Geosciences, **32**, 1411–1419, doi: 10.1016/j.cageo.2006.01.001.

Jones, A. G., 1988, Static shift of magnetotelluric data and its removal in a sedimentary basin environment: Geophysics, **53**, 967–978, doi: 10.1190/1.1442533.

Jones, A. G., 2012, Distortion of magnetotelluric data: Its identification and removal, *in* A. D. Chave and A. G. Jones, eds., The magnetotelluric method, theory and practice: Cambridge University Press, 219–302.

Kennedy, J., and R. Eberhart, 1995, Particle swarm optimization: Proceedings of the IEEE International Conference on Neural Networks, 1942–1948.

Kennett, B. L. N., M. S. Sambridge, and P. R. Williamson, 1988, Subspace methods for large inverse problems with multiple parameter classes: Geophysical Journal, **94**, 237–247, doi: 10.1111/j.1365-246X.1988.tb05898.x.

Kirkpatrick, S., C. D. Gelatt, Jr., and M. P. Vecchi, 1983, Optimization by simulated annealing: Science, **220**, 671–680, doi: 10.1126/science.220.4598.671.

La Torraca, G. A., T. R. Madden, and J. Korringa, 1986, An analysis of the magnetotelluric impedance for three dimensional conductivity structures: Geophysics, **51**, 1819–1829, doi: 10.1190/1.1442228.

Li, M., A. Abubakar, F. Gao, and T. M. Habashy, 2016, Application of the variable projection scheme for calibration in electromagnetic data inversion: IEEE Transactions on Antennas and Propagation, **64**, 332–335, doi: 10.1109/TAP.2015.2498946.

Linde, N., and J. Doetsch, 2016, Joint inversion in hydrogeophysics and near-surface geophysics, in M. Moorkamp, P. Lelievre, N. Linde, and A. Khan, eds., Integrated imaging of the earth: Theory and applications: Wiley Online Library, 119–135.

Marti, A., A. P. Queralt, A. G. Jones, and J. Ledo, 2005, Improving Bahr's invariant parameters using the WAL approach: Geophysical Journal International, **163**, 38–41, doi: 10.1111/j.1365-246X.2005.02748.x.

Meju, M. A., 1996, Joint inversion of TEM and distorted MT soundings: Some effective practical considerations: Geophysics, **61**, 56–65, doi: 10.1190/1.1443956.

Menke, W., 2012, Geophysical data analysis: Discrete inverse theory. MATLAB edition: Elsevier.

Metropolis, N., and S. Ulam, 1949, The Monte Carlo method: The Journal of the Acoustical Society of America, **44**, 335–341.

Moorkamp, M., B. Heincke, M. Jegen, A. W. Roberts, and R. W. Hobbs, 2011, A framework for 3-D joint inversion of MT, gravity and seismic refraction data: Geophysical Journal International, **184**, 477–493, doi: 10.1111/j.1365-246X.2010.04856.x.

Muñoz, G., 2014, Exploring for geothermal resources with electromagnetic methods: Surveys in Geophysics, **35**, 101–122, doi: 10.1007/s10712-013-9236-0.

Pellerin, L., and G. W. Hohmann, 1990, Transient electromagnetic inversion: A remedy for magnetotelluric static shifts: Geophysics, **55**, 1242–1250, doi: 10.1190/1.1442940.

Pethick, A., and B. Harris, 2015, 1D magnetotelluric forward modelling Web App: 24th International Geophysical Conference and Exhibition Perth, ASEG-PESA, Extended Abstracts, 1–4.

Ranieri, G., 2000, Tem-fast: A useful tool for hydro-geologists and environmental engineers: Annals of Geophysics, **43**, 1147–1158, doi: 10.4401/ag-3692.

Rodi, W., and R. L. Mackie, 2001, Nonlinear conjugate gradients algorithm for 2-D magnetotelluric inversion: Geophysics, **66**, 174–187, doi: 10.1190/1.1444893.

Santilano, A., A. Godio, A. Manzella, A. Menghini, E. Rizzo, G. Romano, and A. Viezzoli, 2015, Electromagnetic and DC methods for geothermal exploration in Italy — Case studies and future developments: First Break, **33**, 81–86.

Santilano, A., A. Manzella, E. Rizzo, V. Giampaolo, L. Capozzoli, and A. Godio, 2016, Imaging the deep structures of the Larderello geothermal field (Italy) by electrical resistivity measurements: The IMAGE experiment: Proceedings of the 2016 European Geothermal Congress, 1–5.

Sen, M. K., and P. L. Stoffa, 2013, Global optimization methods in geophysical inversion: Elsevier.

Shaw, R., and S. Srivastava, 2007, Particle swarm optimization: A new tool to invert Geophysical data: Geophysics, **72**, no. 2, F75–F83, doi: 10.1190/1.2432481.

Sims, W. E., and F. X. Bostick, 1969, Methods of magnetotelluric analysis: Technical report 58, University of Texas, Electrical Geophysics Research Laboratory.

Siripunvaraporn, W., 2012, Three-dimensional magnetotelluric inversion: An introductory guide for developers and users: Surveys in Geophysics, **33**, 5–27, doi: 10.1007/s10712-011-9122-6.

Smith, J. T., and J. R. Booker, 1988, Magnetotelluric inversion for minimum structure: Geophysics, **53**, 1565–1576, doi: 10.1190/1.1442438.

Spichak, V. V., 2015, Electromagnetic sounding of the earth's interior, 2nd ed.: Elsevier.

Spichak, V. V., and A. Manzella, 2009, Electromagnetic sounding of geothermal zones: Journal of Applied Geophysics, **68**, 459–478, doi: 10.1016/j.jappgeo.2008.05.007.

Spies, B. R., and F. C. Frischknecht, 1991, Electromagnetic sounding, in M. N. Nabighian, ed., Electromagnetic methods in applied geophysics, vol. 2 — Application, part A: SEG, 285–425.

Sternberg, B. K., J. C. Washburne, and L. Pellerin, 1988, Correction for the static shift in magnetotellurics using transient electromagnetic soundings: Geophysics, **53**, 1459–1468, doi: 10.1190/1.1442426.

Tarantola, A., 2005, Inverse problem theory and methods for model parameter estimation: SIAM.

Tikhonov, A. N., 1950, On determination of electric characteristics of deep layers of the earth's crust: Doklady Akademii Nauk SSSR, **151**, 295–297.

Ward, S. H., and G. W. Hohmann, 1988, Electromagnetic theory for geophysical applications, *in* M. N. Nabighian, ed., Electromagnetic methods in applied geophysics: SEG, 130–311.

Yin, C., 2003, Inherent nonuniqueness in magnetotelluric inversion for 1D anisotropic models: Geophysics, **68**, 138–146, doi: 10.1190/1.1543201.